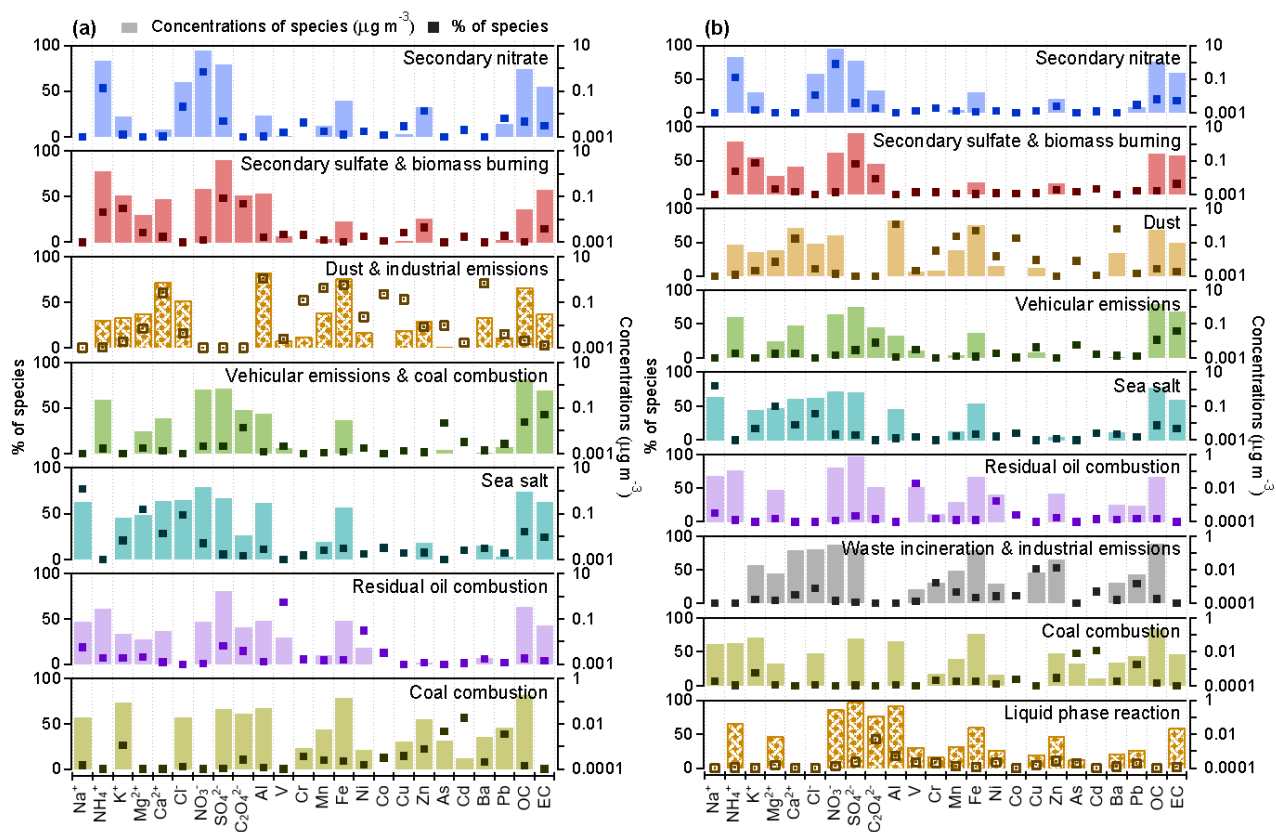
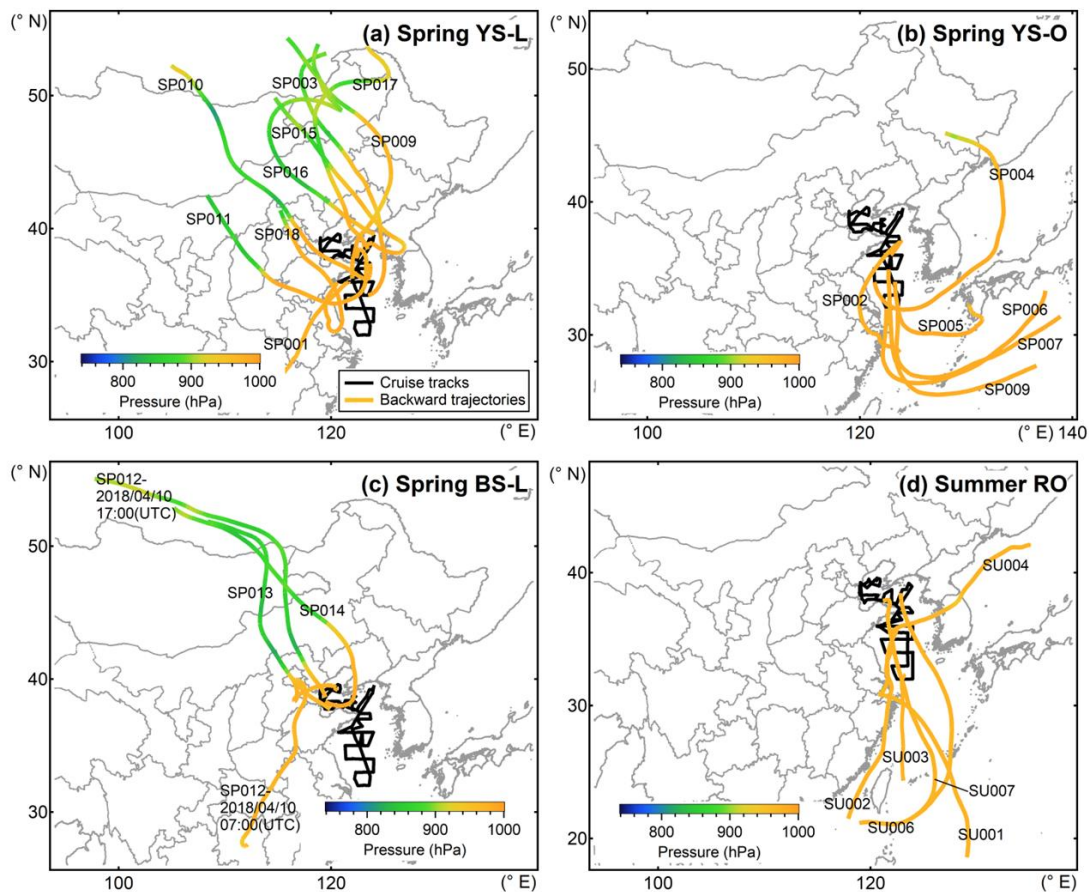


## Supplemental Figures



**Figure S1:** PMF resolved factor profiles (dark points represent the percentages and light rectangles represent the concentrations of each species in each factor) of (a) 7-factor and (b) 9-factor solution.



**Figure S2.** Averaged 72 h backward trajectories arriving at the BS and YS in (a) (b) (c) spring and (d) summer of each sample. The black solid line indicates the cruise tracks. “YS-O” means “YS-ocean”.

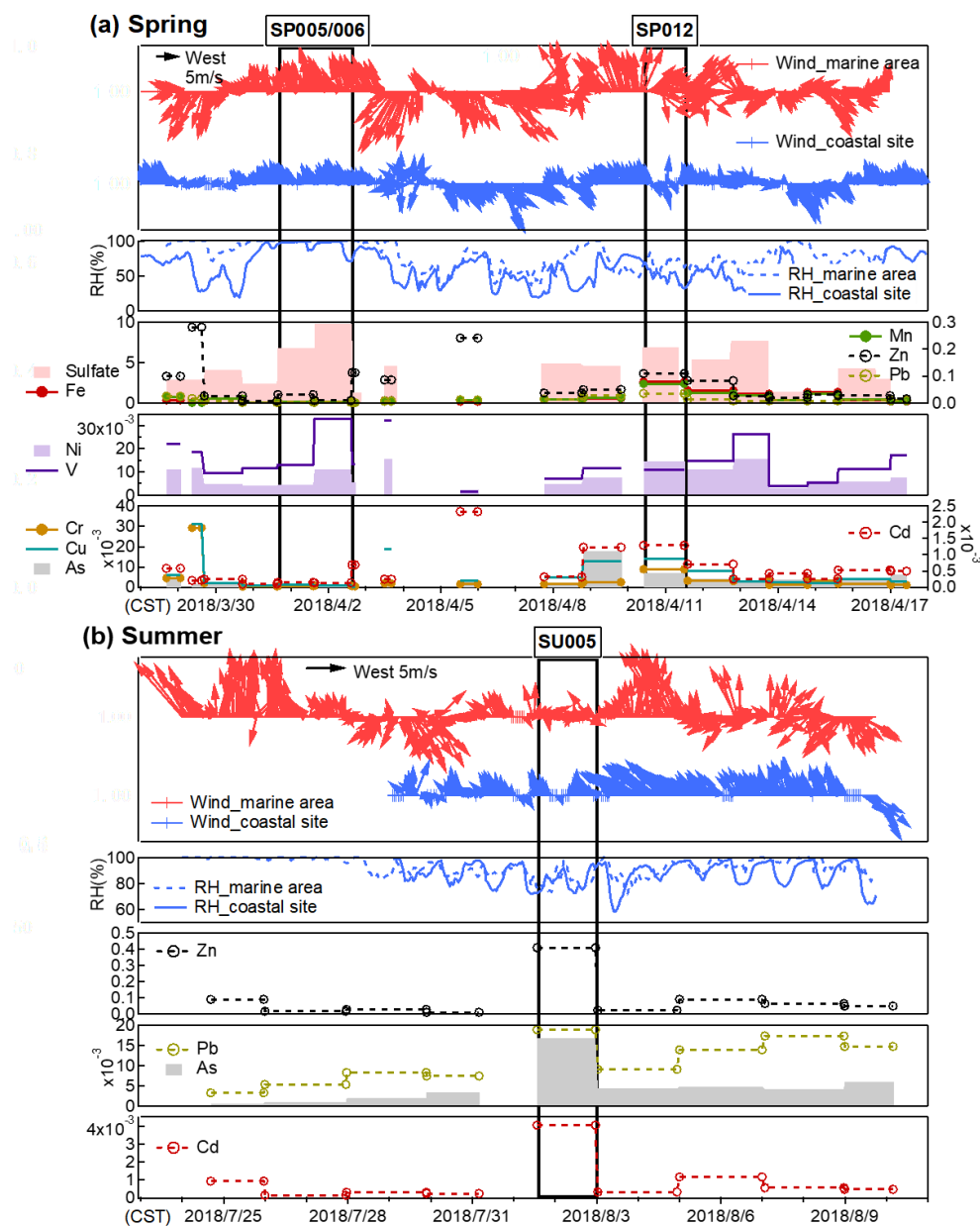


**Figure S3.** Temporal variations of meteorological parameters and selected species concentrations ( $\mu\text{g}/\text{m}^3$ ) in (a) spring and (b) summer. “SP005/006” and “SP012” marked in (a) show the information about the sampling period for sample SP005, SP006, and SP012, respectively. “SU005” marked in (b) shows the sampling period for sample SU005.

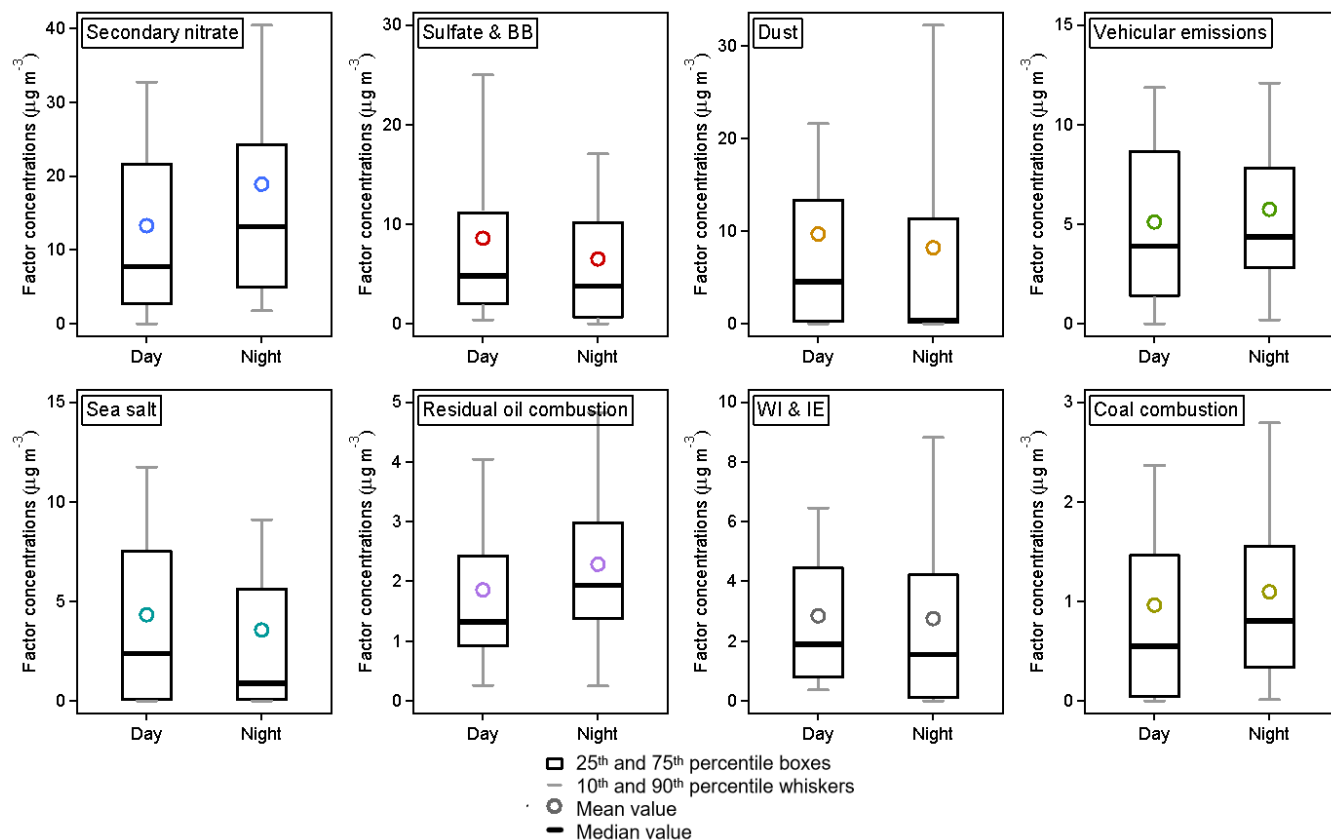


**Figure S4.** Diurnal variations of individual factor contributions from PMF results of spring in Qingdao. (29 daytime and 26 nighttime samples were collected, respectively. 25<sup>th</sup> and 75<sup>th</sup> percentile boxes, 10<sup>th</sup> and 90<sup>th</sup> percentile whiskers; the solid black line is the median value, and the circle is the mean value.) Sulfate & BB represents sulfate & biomass burning. WI & IE represents waste incineration & industrial emissions.

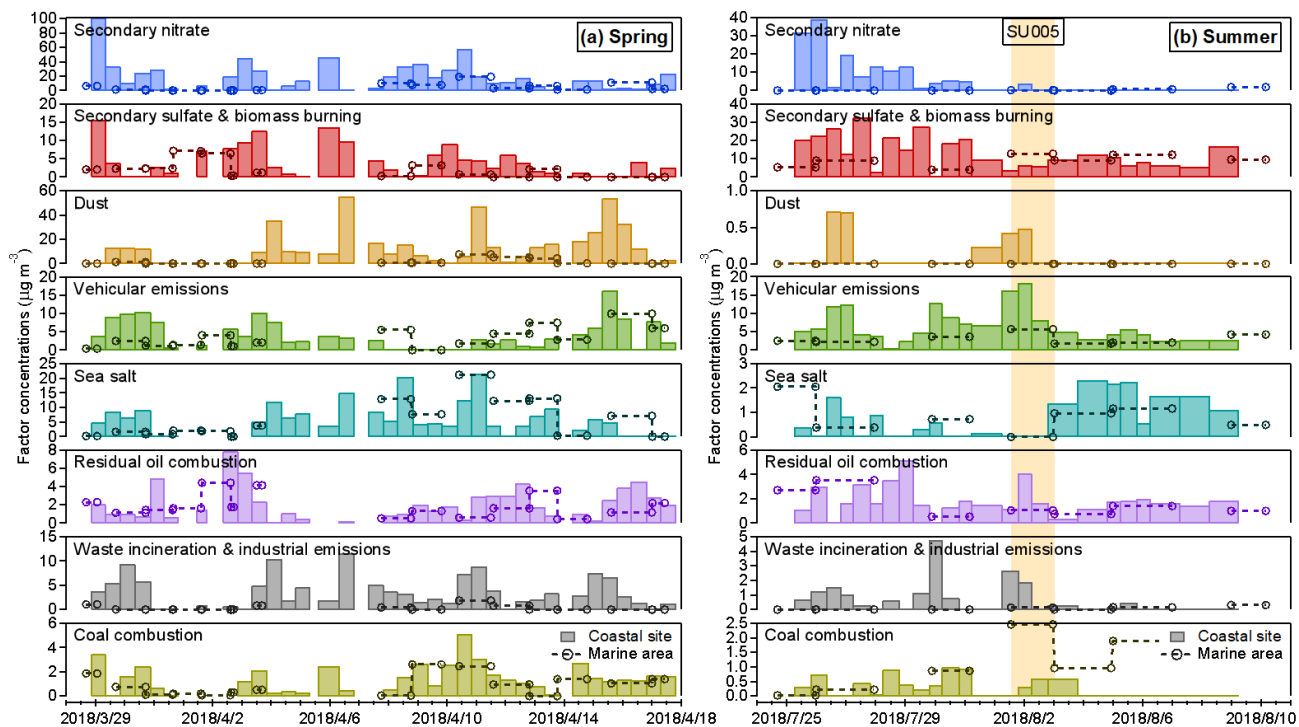


**Figure S5.** Time series of individual PMF factor concentrations for  $PM_{2.5}$  in (a) spring and (b) summer. “SU005” marked in (b) shows the factor concentrations during the sampling period of sample SU005.

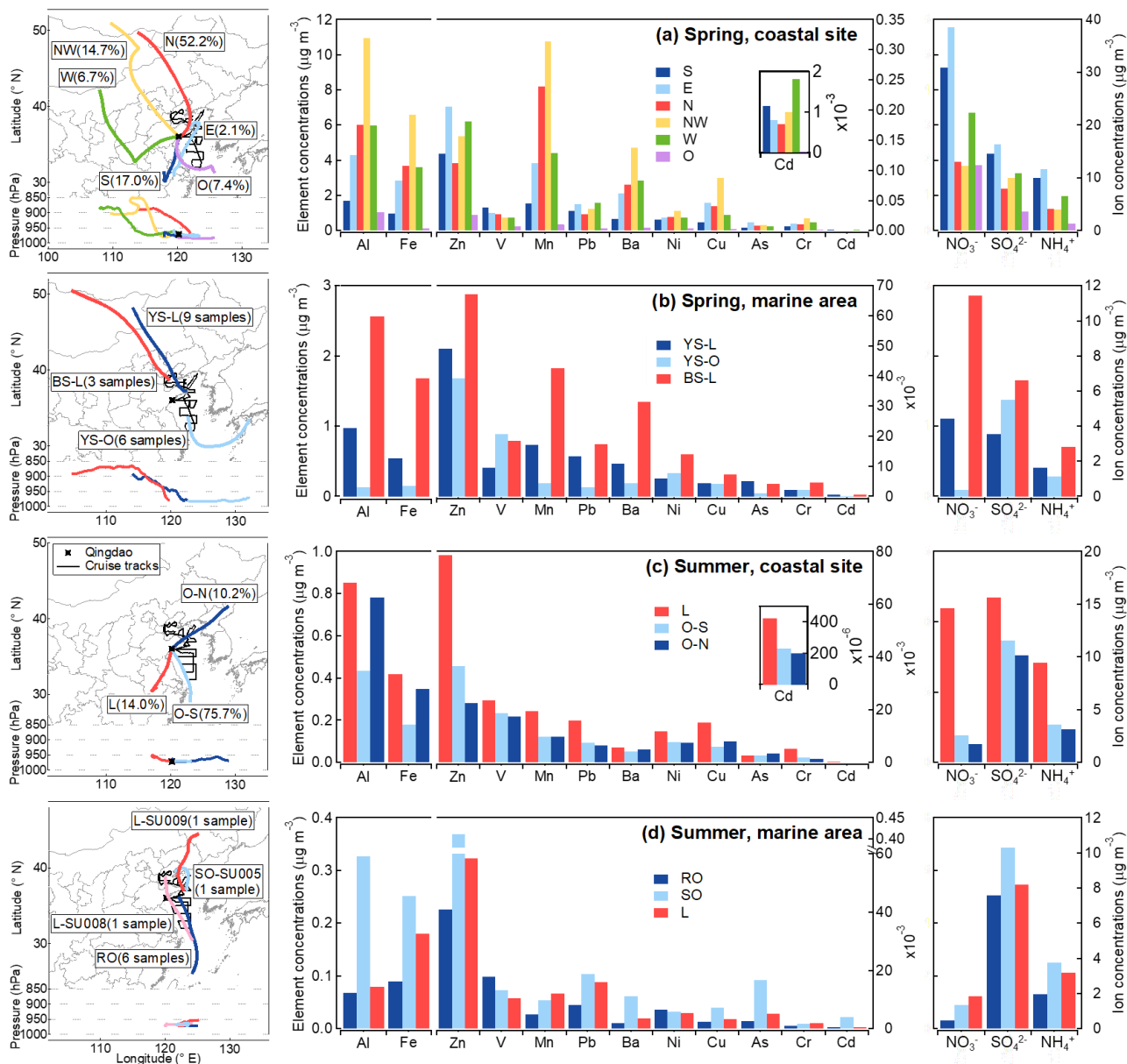


**Figure S6.** To explore the influence of air mass history on variations in trace element abundances, the backward trajectories calculated by HYSPLIT model were classified into six categories in spring and three in summer at the coastal city site, using a systematic clustering method implemented in the software SPSS (Statistical Product and Service Solutions) Statistics v21. For the cruise missions, the trajectory endpoints corresponded to the cruise coordinates, thus the samples were manually classified into three categories in both seasons. Averaged 72 h backward trajectories of air masses arriving at 300 m altitudes and the averaged concentrations of trace elements and ions of individual clusters in spring at (a) the coastal site and (b) offshore and in summer at (c) the coastal site and (d) the offshore area. The black star indicates the coastal site, Qingdao. The solid black line indicates the cruise tracks. “YS-O” means “YS-ocean”. Al and Fe use the left labels, other elements use the right labels.

## Supplemental Tables

**Table S1.** Bootstrap (BS) mapping of 9-factor solution based on PMF.

	Base factor 1	Base factor 2	Base factor 3	Base factor 4	Base factor 5	Base factor 6	Base factor 7	Base factor 8	Base factor 9	Unmapped
Boot factor 1	100	0	0	0	0	0	0	0	0	0
Boot factor 2	0	100	0	0	0	0	0	0	0	0
Boot factor 3	0	0	100	0	0	0	0	0	0	0
Boot factor 4	0	2	1	92	0	0	0	4	0	1
Boot factor 5	0	0	1	0	95	0	1	1	0	2
Boot factor 6	0	0	0	0	0	100	0	0	0	0
Boot factor 7	1	0	12	0	1	0	74*	10	0	2
Boot factor 8	1	0	0	0	0	0	1	98	0	0
Boot factor 9	2	8	13	0	1	0	3	9	58*	6

\*. The mapping percentages were less than 75% using the BS uncertainty method.

**Table S2.** BS mapping of 8-factor solution based on PMF.

	Base factor 1	Base factor 2	Base factor 3	Base factor 4	Base factor 5	Base factor 6	Base factor 7	Base factor 8	Unmapped
Boot factor 1	100	0	0	0	0	0	0	0	0
Boot factor 2	0	99	0	0	0	1	0	0	0
Boot factor 3	0	0	100	0	0	0	0	0	0
Boot factor 4	1	1	0	96	0	0	0	2	0
Boot factor 5	0	0	2	1	93	0	2	1	1
Boot factor 6	0	0	0	0	0	100	0	0	0
Boot factor 7	2	0	10	2	1	0	75	7	3
Boot factor 8	0	0	0	0	0	0	0	100	0

**Table S3.** BS mapping of 7-factor solution based on PMF.

	Base factor 1	Base factor 2	Base factor 3	Base factor 4	Base factor 5	Base factor 6	Base factor 7	Unmapped
Boot factor 1	98	0	0	0	0	1	0	1
Boot factor 2	0	96	1	0	1	1	1	0
Boot factor 3	0	0	100	0	0	0	0	0
Boot factor 4	3	4	8	74*	5	2	3	1
Boot factor 5	1	5	3	1	80	5	4	1
Boot factor 6	0	0	0	0	0	100	0	0
Boot factor 7	1	1	0	0	0	0	98	0

\*. The mapping percentages were less than 75% using the BS uncertainty method.

**Table S4.** Comparison of concentrations ( $\text{ng m}^{-3}$ ) of trace elements over the BS and YS in this study with other studies on  $\text{PM}_{2.5}$  in oceanic regions of China.

Area	Time	Al	Fe	Zn	V	Mn	Pb	Ba	Ni	Cu	As	Cr	Cd	Reference
BS and YS	2018.3–4	1043.2	648.6	49.9	14.2	18.4	11.8	13.0	8.0	5.0	3.7	2.6	0.5	This study
	2018.7–8	93.2	122.0	76.6	16.0	6.8	10.7	3.1	6.3	3.0	4.4	1.4	0.8	
BS	2018.3–4	2562.8	1682.2	67.2	18.5	42.6	17.5	31.5	14.0	7.4	4.1	4.6	0.7	
	2018.7–8	72.6	162.3	79.7	13.1	9.6	15.5	2.9	5.8	3.0	4.6	1.9	0.9	
YS	2018.3–4	689.2	407.9	45.8	13.2	12.8	10.5	8.7	6.6	4.4	3.7	2.1	0.5	
	2018.7–8	99.1	110.4	75.7	16.8	6.0	9.3	3.1	6.5	2.9	4.3	1.2	0.8	
YS	2011.3–4	2803.3	1111.8	74.2	20.7	14.8	18.9	-	20.1	11.5	8.6	-	-	Zhao et al., 2015
ECS	2018.4–5	244.1	223.0	37.9	<b>22.4</b>	10.5	10.6	8.5	<b>8.9</b>	<b>8.0</b>	3.8	<b>14.7</b>	0.3	Sun et al., 2022
Pengjiayu, ECS*	2019.9–2020.8	109.9	71.7	5.7	0.6	1.9	1.5	-	0.4	-	-	-	0.1	Hsieh et al., 2023
Huaniao Island, ECS**	2015–2018	-	160.0	-	-	-	-	-	-	-	-	-	-	Yang et al., 2020
Penghu Islands (PH)	2017.8–9	150	180	40	20	30	40	-	10	20	-	20	<5	Yuan et al., 2023
Dongsha Islands (DS)		80	70	50	<5	10	20	-	<5	20	-	10	<5	
Nansha Islands (NS)***		50	50	30	<5	<5	<5	-	<5	20	-	10	<5	
PH		450	370	150	80	40	100	-	70	30	-	50	30	
DS	2018.3–4	360	310	120	60	30	80	-	60	30	-	40	30	
NS		60	70	40	10	10	50	-	20	10	-	20	20	

\*. The data in this study were derived from particles with aerodynamic diameters less than  $3.1 \mu\text{m}$  ( $\text{PM}_{3.1}$ ).

\*\*. The data in this study were derived from particles with aerodynamic diameters less than  $1.8 \mu\text{m}$  ( $\text{PM}_{1.8}$ ).

\*\*\*. The three remote islands (PH, DS, and NS) were located from the south Taiwan Strait (TS) to the north South China Sea (SCS).



**Table S5.** Comparison of concentrations ( $\text{ng m}^{-3}$ ) of trace elements in Qingdao in this study with other studies on  $\text{PM}_{2.5}$  in typical cities of China.

City	Type	Time	Al	Fe	Zn	V	Mn	Pb	Ba	Ni	Cu	As	Cr	Cd	Reference
Qingdao	Coastal	2018.3–4	5573.5	3347.3	120.1	26.4	188.0	29.3	70.3	21.9	39.5	7.6	11.1	0.8	This study
		2018.7–8	493.8	228.3	40.9	19.2	11.1	8.6	4.4	8.3	7.4	2.7	2.4	0.3	
Qingdao	Coastal	2018.6–7	548.9	347.3	91.7	9.4	~11	22.5	~11	-	-	-	-	-	Li et al., 2018
Qingdao*	Coastal	2019.11–12	935.5	801.0	57.1	2.3	29.9	14.9	19.2	2.5	43.5	2.5	4.3	0.5	Zhang et al., 2021
Beijing	Inland	2005.3–2006.2	790	1130	530	30	90	240	210	20	70	20	50	50	Chen et al., 2008
Tianjin	Coastal	2017.10–2018.8	-	409	136	2	20	31	-	12	33	18	-	-	Zhang et al., 2021
Shanghai	Coastal	2016.3–2017.2	-	410	120	13	32	27	24	6	12	6.6	4.5	9.6	Chang et al., 2018
Shanghai**	Coastal	2004.4–2005.4	-	950	349	9	51	143	12	8	29	28	15	3.7	Chen et al., 2008
Ningbo	Coastal	2014.3–5	1430	1420	229	9.4	-	68.9	-	10.0	20.1	-	14.1	-	Ming et al., 2017
		2014.6–8	676	354	65.3	3.2	-	14.7	-	4.0	4.6	-	9.3	-	
Xiamen	Coastal	2017.1–2018.1	210	290	86.7	10.6	14.3	19.3	11.3	7.1	7.2	1.6	8.5	0.5	Wu et al., 2020
Guangzhou	Coastal	2008.12–2009.2	-	1850	1360	20	150	450	70	-	190	40	70	20	Yang et al., 2011
Hangzhou** *	Near-coastal	2018.11–2020.1	2194.4	2529.1	160.4	2.8	33.2	36.0	59.9	22.1	46.1	-	21.2	-	Zhu et al., 2022

\*. The data in this study were derived from particles with aerodynamic diameters less than  $1 \mu\text{m}$  ( $\text{PM}_{1}$ ).

\*\*. An urban-residential site, Putuo.

\*\*\*. The data were obtained from the analysis using an energy dispersive X-ray fluorescence (EDXRF) spectrometer ( $\text{in } \mu\text{g cm}^{-2}$ ) and have been converted by the authors of this study ( $\text{in ng m}^{-3}$ ).

**Table S6.** Pearson correlations (r) of PMF factor contributions with meteorological parameters (relative humidity (RH) and wind speed (WS)), and gas pollutants concentrations (SO<sub>2</sub>, NO<sub>2</sub>, O<sub>3</sub> and CO).

Factor	RH	WS	SO <sub>2</sub>	NO <sub>2</sub>	O <sub>3</sub>	CO
Secondary nitrate	-0.23	-0.16	0.32*	0.47**	0.26*	0.37**
Secondary sulfate & biomass burning	0.39**	-0.26*	-0.39**	-0.45**	0.36**	0.55**
Dust	-0.72**	0.23	0.19	0.34**	-0.11	-0.13
Dust (spring, coastal)	-	0.42*	-	-	-	-
Vehicular emissions	-0.07	-0.40**	0.04	0.06	-0.35**	0.32*
Vehicular emissions (summer)	-0.47	-0.57*	0.63**	0.82**	-0.15	0.35
Sea salt	-0.58**	0.39**	0.31*	0.47**	-0.04	-0.02
Residual oil combustion	0.15	-0.17	0.40**	0.17	-0.02	0.00
Waste incineration & Industrial emissions	-0.69**	0.05	0.29*	0.52**	-0.17	0.03
Coal combustion	-0.23	-0.05	0.39**	0.59**	0.12	0.22

Note. The highest correlation coefficients for each factor are denoted in bold. No gas pollutants data was available for the cruise campaign. The meteorological parameters of the former eight samples in summer are missing values.

\*. Correlation is significant at the 0.05 level (2-tailed).

\*\*. Correlation is significant at the 0.01 level (2-tailed).

**Table S7.** The information of averaged 72 h air mass backward trajectory clusters arriving at the coastal site and marine area in spring and summer.

Campaign	Cluster	Detailed information	Frequency
Spring, coastal site	N (North)	From the north and passed the Inner Mongolia Autonomous region and Liaoning Province	52.2%
	NW (Northwest)	From the northwest and passed the Inner Mongolia Autonomous and BTH region	14.7%
	W (West)	From the Inner Mongolia Autonomous region and passed Shaanxi and Henan Provinces	6.7%
	S (South)	From East China near the Yangtze River Delta (YRD)	17.0%
	E (East)	From East China near YRD and passed YS before reversing to the Shandong Peninsula	2.1%
	O (Ocean)	Mainly from ECS and passed YS	7.4%
Spring, marine area	BS-L (BS-Land)	BS samples influenced by the continent air masses	Three samples
	YS-L (YS-Land)	YS samples influenced by the continent air masses	Nine samples
	YS-O (YS-Ocean)	YS samples influenced by the marine air masses	Six samples
Summer, coastal site	L (Land)	Passed the continent of East China before arriving at QD	14.0%
	O-S (Ocean-South)	From ECS in the south	75.7%
	O-N (Ocean-North)	From Korean Peninsula in the north	10.2%
Summer, marine area	L (Land)	Two samples influenced by the continent air masses, one passed the coastline of southeastern China (L-SU008), another from the northern China (L-SU009)	Two samples
	RO (Remote oceans)	Samples influenced by remote ocean air masses	Six samples
	SO (Surrounding oceans)	BS sample influenced by the air masses lingered over the CBS region	One sample, SU005

**Table S8.** Percentage contributions (%) of various source factors to individual elements based on PMF.

Element	Season	location	Secondary nitrate	Sulfate &BB	Dust	VE	Sea salt	ROC	WI&IE	CC
Fe	Spring	Coastal	1.6	0.2	77.8	1.2	1.8	1.9	9.6	5.8
		Marine	2.4	0.6	45.5	6.7	11.3	10.0	3.8	19.7
	Summer	Coastal	5.2	8.7	6.4	21.8	3.5	21.2	19.6	13.6
		Marine	0.4	5.8	0	10.4	2.9	19.5	2.7	58.3
Mn	Spring	Coastal	3.2	0.7	67.9	1.4	1.2	1.8	18.0	5.9
		Marine	4.7	2.0	40.5	7.9	7.9	9.5	7.2	20.3
	Summer	Coastal	7.2	19.4	4.0	18.0	1.7	14.0	26.0	9.8
		Marine	0.6	15.7	0	10.4	1.7	15.8	4.5	51.2
Cr	Spring	Coastal	9.5	2.3	46.1	0.4	0.1	2.7	31.0	7.8
		Marine	13.4	6.7	26.1	2.2	0.8	13.4	11.8	25.6
	Summer	Coastal	12.3	38.2	1.5	3.0	0.1	11.9	25.6	7.4
		Marine	1.2	34.2	0	1.9	0.1	14.8	4.8	42.9
Ni	Spring	Coastal	4.5	2.5	39.2	2.4	2.0	23.3	22.5	3.7
		Marine	3.2	3.7	11.2	6.5	6.4	58.6	4.3	6.1
	Summer	Coastal	3.0	21.5	0.7	9.1	0.8	53.4	9.6	1.8
		Marine	0.3	18.3	0	5.6	0.9	63.3	1.7	9.9
V	Spring	Coastal	5.9	3.8	0	3.8	0	56.3	30.1	0
		Marine	2.5	3.4	0	6.2	0	84.4	3.5	0
	Summer	Coastal	2.1	17.1	0	7.6	0	66.6	6.6	0
		Marine	0.2	14.6	0	4.6	0	79.3	1.2	0
Cu	Spring	Coastal	1.4	0.7	15.3	7.6	0	0.7	70.1	4.2
		Marine	2.1	2.0	8.9	42.0	0	3.6	27.4	14.1
	Summer	Coastal	1.4	8.3	0.4	41.7	0	2.3	43.0	2.9
		Marine	0.2	11.8	0	42.9	0	4.7	13.1	27.4
Zn	Spring	Coastal	16.6	5.0	0	0	7.4	2.4	55.4	13.1
		Marine	14.6	9.1	0	0	28.9	7.4	13.2	26.9
	Summer	Coastal	12.0	46.3	0	0	3.3	5.8	25.5	6.9
		Marine	1.2	41.9	0	0	3.8	7.4	4.9	40.8
Cd	Spring	Coastal	4.5	4.3	6.0	2.7	15.0	0.8	15.1	51.7
		Marine	2.0	4.0	1.1	4.7	30.2	1.3	1.9	54.8
	Summer	Coastal	3.3	40.8	0.1	11.4	6.9	2.1	7.2	28.2
		Marine	0.1	16.6	0	3.3	3.6	1.2	0.6	74.5
Pb	Spring	Coastal	15.7	4.0	8.7	1.2	8.8	1.6	29.4	30.7
		Marine	10.1	5.2	2.2	2.9	24.9	3.7	5.1	45.9
	Summer	Coastal	12.5	40.4	0.2	5.4	4.3	4.4	14.9	17.9
		Marine	0.8	22.9	0	2.2	3.1	3.5	1.8	65.8
As	Spring	Coastal	0	1.4	36.4	13.0	0	0	2.7	46.5
		Marine	0	1.6	8.3	28.3	0	0	0.4	61.4
	Summer	Coastal	0	13.8	0.7	57.8	0	0	1.4	26.4
		Marine	0	6.1	0	18.3	0	0	0.1	75.5

Note. Sulfate&BB represents sulfate & biomass burning. VE represents vehicular emissions. ROC represents residual oil combustion. WI&IE represents waste incineration & industrial emissions. CC represents coal combustion.

## References

- Chang, Y., Huang, K., Xie, M., Deng, C., Zou, Z., Liu, S., and Zhang, Y.: First long-term and near real-time measurement of trace elements in China's urban atmosphere: Temporal variability, source apportionment and precipitation effect. *Atmos. Chem. Phys.*, 18, 11793-11812. <https://doi.org/10.5194/acp-18-11793-2018>, 2018.
- Chen, J., Tan, M., Li, Y., Zheng, J., Zhang, Y., Shan, Z., Zhang, G., and Li, Y.: Characteristics of trace elements and lead isotope ratios in PM<sub>2.5</sub> from four sites in Shanghai, *J. Hazard. Mater.*, 156, 36-43, <https://doi.org/10.1016/j.jhazmat.2007.11.122>, 2008.
- Hsieh, C. -C., You, C. -F., & Ho, T. -Y.: The solubility and deposition flux of East Asian aerosol metals in the East China Sea: The effects of aeolian transport processes. *Mar. Chem.*, 253, 104268. <https://doi.org/10.1016/j.marchem.2023.104268>, 2023.
- Li, P., Li, Q., Shi, J., Gao, H., and Yao, X.: Concentration, solubility, and dry deposition flux of trace elements in fine and coarse particles in Qingdao during summer (in Chinese), *Environ. Sci.*, 39, 3067-3074, <https://doi.org/10.13227/j.hjlx.201712231>, 2018.
- Ming, L., Jin, L., Li, J., Fu, P., Yang, W., Liu, D., Zhang, G., Wang, Z., and Li, X.: PM<sub>2.5</sub> in the Yangtze River Delta, China: Chemical compositions, seasonal variations, and regional pollution events. *Environ. Pollut.*, 223, 200-212. <https://doi.org/10.1016/j.envpol.2017.01.013>, 2017.
- Sun, H., Sun, J., Zhu, C., Yu, L., Lou, Y., Li, R., and Lin, Z.: Chemical characterizations and sources of PM<sub>2.5</sub> over the offshore Eastern China sea: Water soluble ions, stable isotopic compositions, and metal elements. *Atmos. Pollut. Res.*, 13, 101410. <https://doi.org/10.1016/j.apr.2022.101410>, 2022.
- Wu, S. P., Cai, M. J., Xu, C., Zhang, N., Zhou, J. B., Yan, J. P., Schwab, J. J., and Yuan, C. S.: Chemical nature of PM<sub>2.5</sub> and PM<sub>10</sub> in the coastal urban Xiamen, China: Insights into the impacts of shipping emissions and health risk, *Atmos. Environ.*, 227, <https://doi.org/10.1016/j.atmosenv.2020.117383>, 2020.
- Yang, F., Tan, J., Zhao, Q., Du, Z., He, K., Ma, Y., Duan, F., Chen, G., and Zhao, Q.: Characteristics of PM<sub>2.5</sub> speciation in representative megacities and across China, *Atmos. Chem. Phys.*, 11, 5207-5219, <https://doi.org/10.5194/acp-11-5207-2011>, 2011.
- Yang, T., Chen, Y., Zhou, S., Li, H., Wang, F., and Zhu, Y.: Solubilities and deposition fluxes of atmospheric Fe and Cu over the Northwest Pacific and its marginal seas, *Atmos. Environ.*, 239, 117763, <https://doi.org/10.1016/j.atmosenv.2020.117763>, 2020.
- Yuan, C. -S., Hung, C. -M., Hung, K. -N., Yang, Z. -M., Cheng, P. -H., and Soong, K. -Y.: Route-based chemical significance and source origin of marine PM<sub>2.5</sub> at three remote islands in East Asia: Spatiotemporal variation and long-range transport. *Atmos. Pollut. Res.*, 14, 101762. <https://doi.org/10.1016/j.apr.2023.101762>, 2023.
- Zhang, H., Li, R., Dong, S., Wang, F., Zhu, Y., Meng, H., Huang, C., Ren, Y., Wang, X., Hu, X., Li, T., Peng, C., Zhang, G., Xue, L., Wang, X., and Tang, M.: Abundance and Fractional Solubility of Aerosol Iron During Winter

at a Coastal City in Northern China: Similarities and Contrasts Between Fine and Coarse Particles, *J. Geophys. Res.-Atmos.*, 127, <https://doi.org/10.1029/2021JD036070>, 2022.

Zhang, W., Peng, X., Bi, X., Cheng, Y., Liang, D., Wu, J., Tian, Y., Zhang, Y., and Feng, Y.: Source apportionment of PM<sub>2.5</sub> using online and offline measurements of chemical components in Tianjin, China. *Atmos. Environ.*, 244, 117942. <https://doi.org/10.1016/j.atmosenv.2020.117942>, 2021.

Zhao, R., Han, B., Lu, B., Zhang, N., Zhu, L., and Bai, Z.: Element composition and source apportionment of atmospheric aerosols over the China Sea. *Atmos. Pollut. Res.*, 6, 191-201. <http://doi.org/10.5094/APR.2015.023>, 2015.

Zhu, Y., Li, W., Wang, Y., Zhang, J., Liu, L., Xu, L., Xu, J., Shi, J., Shao, L., Fu, P., Zhang, D., and Shi, Z.: Sources and processes of iron aerosols in a megacity in Eastern China, *Atmos. Chem. Phys.*, 22, 2191-2202. <https://doi.org/10.5194/acp-22-2191-2022>, 2022.